J. Plant Biol. (2019) 62:451-462
DOI 10.1007/s12374-019-0480-9

RESEARCH ARTICLE

Alteration of Carotenoid Metabolic Machinery by β-Carotene Biofortification in Rice Grains

Hyung-Keun Ku[1,†], Ye Sol Jeong[1,†], Min Kyoung You[1], Young Joo Jung[1], Tae Jin Kim[2], Sun-Hyung Lim[3], Jae Kwang Kim[2,*] and Sun-Hwa Ha[1,*]

[1]*Department of Genetic Engineering and Graduate School of Biotechnology, College of Life Sciences, Kyung Hee University, Yongin 17104, Korea*
[2]*Division of Life Sciences and Bio-Resource and Environmental Center, Incheon National University, Incheon 22012, Korea*
[3]*National Academy of Agricultural Science, Rural Development Administration, Jeonju 54874, Korea*

Received: November 5, 2019 / Accepted: November 13, 2019

Abstract To increase nutritional values as dietary sources of provitamin A and health-promoting antioxidants in rice grains, carotenoids have been biofortified in a Golden Rice-like variety, the *stPAC* (*stPsy-2A-stCrtI*) rice. In both of non-transgenic (NT) and *stPAC* seeds, total chlorophylls and carotenoids were gradually decreased during seed development while *de novo* biosynthesized carotenoids being comprised mainly of β-carotene, lutein and zeaxanthin were accumulated from early stage of 10 DAF and peaked at 20 DAF in *stPAC* seeds. The *de novo* production of carotenoids coincided with the high levels of transgene expression driven by the rice globulin gene promoter. Interestingly, expression levels of endogenous carotenoid metabolic pathway genes were the highest at 30 DAF in NT seeds whereas they were generally down-regulated in *stPAC* seeds, suggesting a negative feed-back control mechanism of carotenoid metabolism by enhanced carotenoid production. The transgenic protein levels in *stPAC* seeds were not changed much during seed storage for up to 5 years, while carotenoid contents in the seeds were decreasing after 1 year of storage. The decrease in carotenoid contents was restored when the transgenic plants re-grown, supporting the reliability of transgenic pathways for carotenoid biofortification in rice grains. Thus, our results showed that transgene-driven biofortification of carotenoids was made and maintained over several transgenic generations with a possible negative feed-back control of endogenous carotenoid metabolism during seed development.

Key words: Biofortification, Carotenoid, Golden rice, Grain, Pedigree, Storage

Introduction

Carotenoids, C_{40} terpenoids, are natural lipophilic pigments synthesized *de novo* in all photosynthetic organisms and several non-photosynthetic bacteria and fungi (Rodriguez-Concepcion et al. 2018). Plant carotenoids are produced and accumulated in plastids and play important roles as photosynthetic accessory pigments and photoprotectants (Hashimoto et al. 2016; Emiliani et al. 2018). As effective antioxidants that interact with free radicals and singlet oxygen, carotenoids are beneficial to human health (Fiedor and Burda 2014). As is well known (Rodriguez-Concepcion, et al. 2018), the central carotenoid pathway begins with phytoene (C_{40}), a colorless carotenoid, as the precursor of downstream colored carotenoids (Fig. 1). The upstream pathway supplies the main substrate of geranylgeranyl diphosphate (GGPP, C_{20}) via the 2-C-methyl D-erythritol 4-phosphate (MEP) pathway, which consists of an initial condensation step of D-glyceraldehyde 3-phosphate (G3P, C_3) and pyruvate (C_3) into 1-deoxy-D-xylulose 5-phosphate (DXP, C_5); the following six conversion steps into MEP (C_5), 4-diphosphocytidyl-2-C-methyl-D-erythritol (C_{14}), 4-diphosphocytidyl-2-C-methyl-D-erythritol 2-phosphate (C_{14}), 2-C-methyl-D-erythritol-2,4-cyclodiphosphate (C_5), 4-hydroxy-3-methylbut-2-enyl diphosphate (C_5), and dimethylallyl diphosphate (DMAPP, C_5)/its double-bond isomer isopentenyl diphosphate (IPP, C_5); and the final condensation step between one DMAPP and three IPPs into GGPP, the common precursor for carotenoids and diterpenoids, including the phytohormone gibberellic acid (GA, C_{19}). In the main carotenoid biosynthetic pathway,

[†]These authors contributed equally to this work.

*Corresponding author; Jae Kwang Kim, Sun-Hwa Ha
Tel : +82-32-835-8241, +82-31-201-2654
E-mail : kjkpj@inu.ac.kr, sunhwa@khu.ac.kr

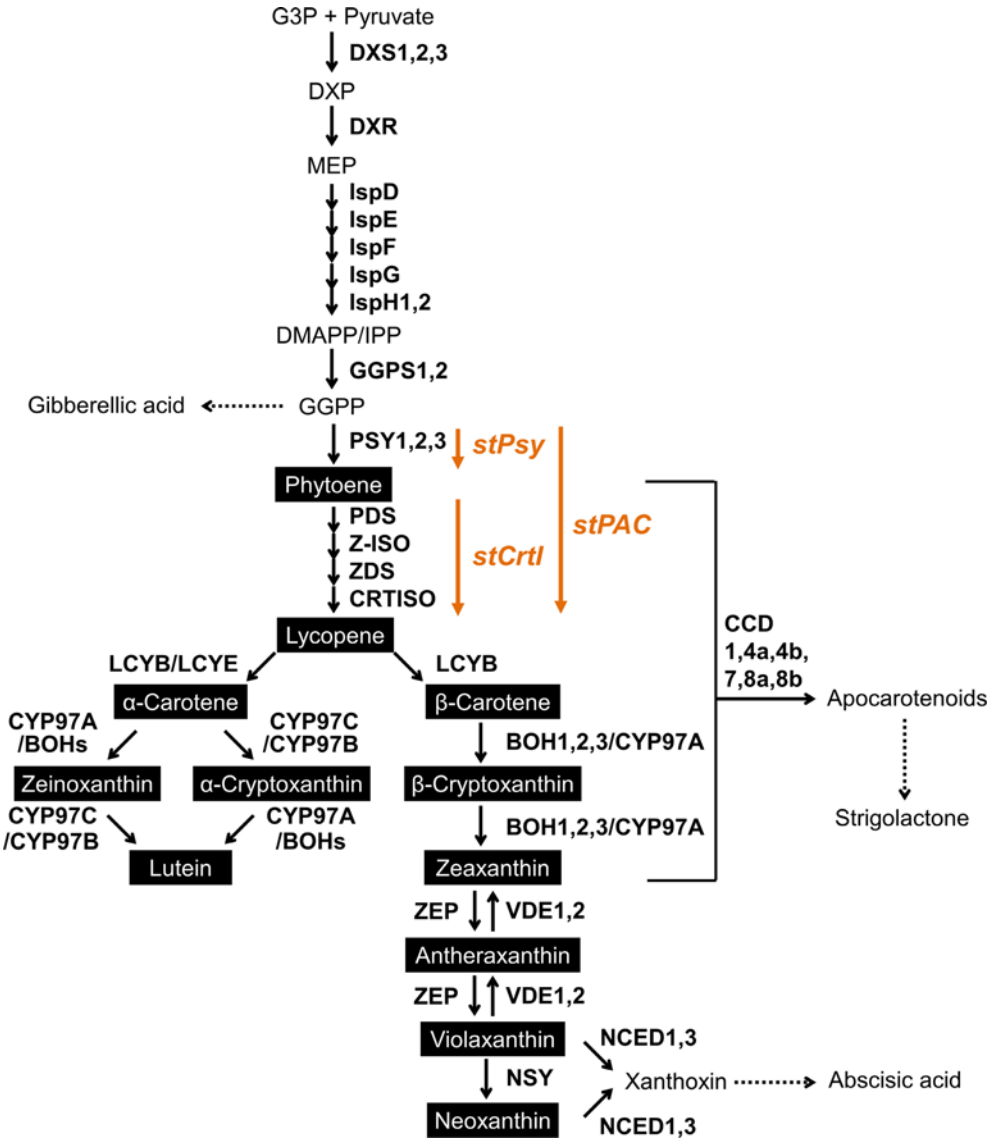

Fig. 1. Schematic overview of carotenoid biosynthetic pathway and metabolic engineering steps implemented in this study. The endogenous MEP and carotenoid pathways found in plant species are localized in the plastids. Solid and dashed arrows represent single or multiple enzymatic steps, respectively. Enzymes are indicated in bold. Carotenoid metabolites are black-boxed in white. The transgenes used in this study, *stPsy, stCrtI* and *stPAC*, are shown in orange with orange arrows representing in the corresponding enzymatic steps. G3P, glyceraldehyde-3-phosphate; DXS, 1-deoxy-d-xylulose-5-phosphate synthase; DXP, 1-deoxy-d-xylulose-5-phosphate; DXR, 1-D-deoxy-d-xylulose 5-phosphate reductoisomerase; MEP, 2-C-methyl-D-erythritol-4-phosphate; IspD, 2-C-methyl-D-erythritol-4-phosphate cytidylyltransferase; IspE, 4-diphosphocytidyl-2-C-methyl-D-erythritol kinase; IspF, 2-C-methyl-D-erythritol-2,4-cyclodiphosphate synthase; IspG, 1-hydroxy-2-methyl-2-(E)-butenyl-4-diphosphate synthase; IspH, 4-hydroxy-3-methyl-2-(E)-butenyl-4-diphosphate reductase; DMAPP, dimethylallyl diphosphate; IPP, isopentenyl diphosphate; GGPS, GGPP synthase; GGPP, geranylgeranyl diphosphate; PSY, phytoene synthase; PDS, phytoene desaturase; Z-ISO, ζ-carotene isomerase; ZDS, ζ-carotene desaturase; CRTISO, carotenoid isomerase; LCYB, lycopene β-cyclase; LCYE, lycopene ε-cyclase; CYP97A, P450-type β-ring hydroxylase; CYP97B, P450-type ε-ring hydroxylase; CYP97C, P450-type ε-ring hydroxylase; BOH, beta-carotene hydroxylase; ZEP, zeaxanthin epoxidase; VDE, violaxanthin deepoxidase; NSY, neoxanthin synthase; NCED, 9-cis-epoxycarotenoid dioxygenase; CCD, carotenoid cleavage dioxygenase.

phytoene is converted into lycopene (C_{40}), a non-cyclic linear carotenoid, through alternate reactions between two desaturations and two isomerizations. Lycopene then bifurcates into α-carotene (C_{40}) or β-carotene (C_{40}) by cyclization to form an α-/β-ring or a β-/β-ring at the end, respectively. Hydroxylation steps then convert α-carotene into α-xanthophylls (C_{40}), including zeinoxanthin, α-cryptoxanthin and lutein, and β-carotene into β-xanthophylls (C_{40}), including β-cryptoxanthin and zeaxanthin. Zeaxanthin is further converted into antheraxanthin (C_{40}) and violaxanthin (C_{40}) by epoxidation at

both ends; these products can be switched back to zeaxanthin by deepoxidation. Violaxanthin and its epoxide-opening isomer neoxanthin (C_{40}) can also be cleaved into xanthoxin (C_{15}), a precursor for the phytohormone abscisic acid (ABA, C_{15}). Carotenoids can also be cleaved at different double-bond positions to produce diverse apocarotenoids, including the phytohormone strigolactones (Hou et al. 2016).

In terms of nutritional value, carotenoids are precursors of vitamin A and help prevent diseases such as blindness and impairment of the immune system (Eggersdorfer and Wyss 2018). Human intake usually relies on diverse carotenoid-rich leaves, fruits and root vegetables. However, in developing countries, which are highly dependent on staple foods, meeting minimum nutritional requirements may rely on carotenoid biofortification by metabolic engineering in common staple crops (Fitzpatrick et al. 2012; Badejo 2018). The first successful example of this was achieved in Golden Rice (GR) 1 by expression of the two β-carotene biosynthetic genes, *Narcissus pseudonarcissus* phytoene synthase (*NpPsy*) and *Pantoea ananatis* carotene desaturase (*PaCrtI*) (Ye et al. 2000). Since then, β-carotene as a main provitamin A component has been remarkably enhanced in GR2 (Paine et al. 2005) and biofortified in other staple crops like potato (*Solanum tuberosum*) (Diretto et al. 2007), maize (*Zea mays*) (Zhu et al. 2008), cassava (*Manihot esculenta*) (Sayre et al. 2011) and wheat (*Triticum aestivum*) (Zeng et al. 2015). Moreover, GR varieties have been diversified with a *PAC* (*CaPsy-2A-PaCrtI*) rice using a single recombinant gene by adopting a 2A-bicistronic system to simultaneously express *Capsicum annuum Psy* (*CaPsy*) and the bacterial *CrtI* (Ha et al. 2010). The codon-optimized synthetic version, *stPAC* (*stPsy-2A-stCrtI*) rice, resulted in 4- and 2.9-fold enhanced levels of β-carotene and total carotenoids, respectively (Jeong et al. 2017). Recently, novel rice varieties displaying yellow, pinkish-red and orange-red coloration due to the accumulation of zeaxanthin, astaxanthin and capsanthin have been created by combining the bicistronic 2A system, multi-cassette incorporation and conventional breeding for effective multi-step metabolic engineering and biochemical pathway extension (Ha et al. 2019).

Plants have different mechanisms for synthesis, accumulation, regulation and degradation of carotenoids between photosynthetic leaves and non-photosynthetic fruits, roots/tubers, flowers and grains. Carotenoid metabolism has been intensively examined among comparable cultivars showing different color phenotypes in carotenoid-rich fruit crops (CFraser et al. 1994; Li et al. 2015; Karppinen et al. 2016; Cao et al. 2017; Hadjipieri et al. 2017). During fruit development and ripening, the expression profiles of relevant carotenoid genes and metabolites were compared in two peach (*Prunus persica*) cultivars (Cao et al. 2017), bilberry (*Vaccinium myrtillus*) under different light conditions(Karppinen et al. 2016), four watermelon (*Citrullus lanatus*) cultivars (Li et al. 2015), tomato (*Lycopersicon esculentum*) with two stages of leaves, flowers and roots (Fraser et al. 1994) and loquat (*Eriobotrya japonica*) peel and flesh tissue (Hadjipieri et al. 2017). The results of these studies indicated that differential transcriptional regulation of carotenoid metabolic genes may be the main mechanism in determining the amount and type of specific carotenoids accumulated in different stages and conditions in fruits.

Likewise, during grain development in cereal crops, wheat carotenoids with resembling composition of photosynthetic tissues progressively decreased from early to mature stages when tetraploid durum wheat (*T. turgidum*, yellow grain) and hexaploid bread wheat (*T. aestivum*, white grain) were compared to show differentially regulated carotenoid metabolic genes at the transcriptional level (Qin et al. 2016). Unlike wheat, yellow-endosperm sorghum (*Sorghum bicolor*) showed a peak accumulation of total carotenoids in the middle stage of grain development with an increase from 10 to 30 days after half bloom (DAHB) and then a decline from 30 to 50 DAHB in developing kernels (Kean et al. 2007). Without carotenoid metabolite profiles during seed development of rice (*Oryza sativa*), carotenoid biosynthetic genes have been examined by qRT-PCR in two stages of developing and mature seeds and analyzed further at five stages with a publicly available microarray database (the Gene Expression Omnibus) (Chaudhary et al. 2010). These results showed that most carotenoid genes were down-regulated as ripening progressed. Particularly in transgenic rice, carotenoid-biofortified seeds have been examined for expression of endogenous carotenoid biosynthetic genes in the immature milky-stage endosperm of GR (*NpPsy/PaCrtI*) (Schaub et al. 2005) and the mature endosperm of L (*ZmPsy/PaCrtI*), D (*AtDxs/ZmPsy/PaCrtI*) and O (*AtOr/ZmPsy/PaCrtI*) lines (Bai, et al. 2016). While the GR and L lines did not show up-regulation of the endogenous rice pathway in response to the transgenes, the D and O lines showed differing up-regulation. The proteome and metabolome of mature seeds of GR lines with the Asian rice cultivar BR29 have also been analyzed (Gayen et al. 2016), revealing altered carbohydrate metabolism, including enhanced pyruvate biosynthesis, after enhancement of carotenoid biosynthesis via a metabolic adaptation process. Only one study in maize has examined the interactions between introduced and native carotenoid pathways during endosperm development by targeted transcriptomic and metabolic profiling (Farr et al. 2013). Taken together, the results from other cereal crops suggest that the native carotenoid metabolic pathway in rice is similar to wheat and quite different from sorghum and maize. This raised the question of how the transgenic carotenoid biosynthetic pathway affects the endogenous carotenoid metabolic pathway during rice seed development. To understand transgene influence, we investigated

changes in eight carotenoid profiles and examined the expression of 38 endogenous carotenogenic genes between NT and *stPAC* rice grains at five stages during development. In addition, we evaluated the levels of transgene translation and carotenoid contents in eight sequential pedigrees of *stPAC* seeds to ascertain the stability of carotenoid metabolites and their production machinery.

Results and Discussion

Morphological and Chemical Phenotypes in NT and *stPAC* Rice Grains

To define how carotenoid biofortification influenced rice grain phenotypes, seed samples were collected at 5, 10, 15, 20, 30 and 40 days after flowering (DAF) as grain-filling progressed in the field. In both NT and *stPAC* rice, seed size was gradually increased up to 20 DAF until fully developed and then remained constant (Fig. 2A). Seed weight was also similar between varieties in fresh (from 15 to 25 mg/seed FW) and dry (from 5 to 20 mg/seed DW) conditions with gradually reduced water content in NT (from 62% to 21%) and *stPAC* (from 65% to 24%) seeds (Fig. S1). Germination rates were evaluated between NT and *stPAC* seeds, considering that carotenoids share a substrate as a competitor to GA and supply precursors for ABA (Fig. 2B). A lack of significant difference indicated that carotenoid biofortification in a seed-specific manner does not affect the balance between GA and ABA.

Meanwhile, coloration was similarly green in the early stages between NT and *stPAC* seeds until 20 DAF and then varied considerably between white (NT) and yellow (*stPAC*) after 30 DAF due to green decreasing in both and yellow increasing only in *stPAC* (Fig. 2A). These color phenotypes are attributed to the amounts of two color pigments, chlorophylls and carotenoids (Fig. 2C, D). Chlorophylls gradually decreased from the earliest stage showing the highest level, sharply declined between 20 and 30 DAF and completely disappeared at 40 DAF in grains of both varieties. Carotenoids, in relatively high levels from 10 to 15 DAF, also gradually declined until 40 DAF with a sharp decrease between 20 and 30 DAF in

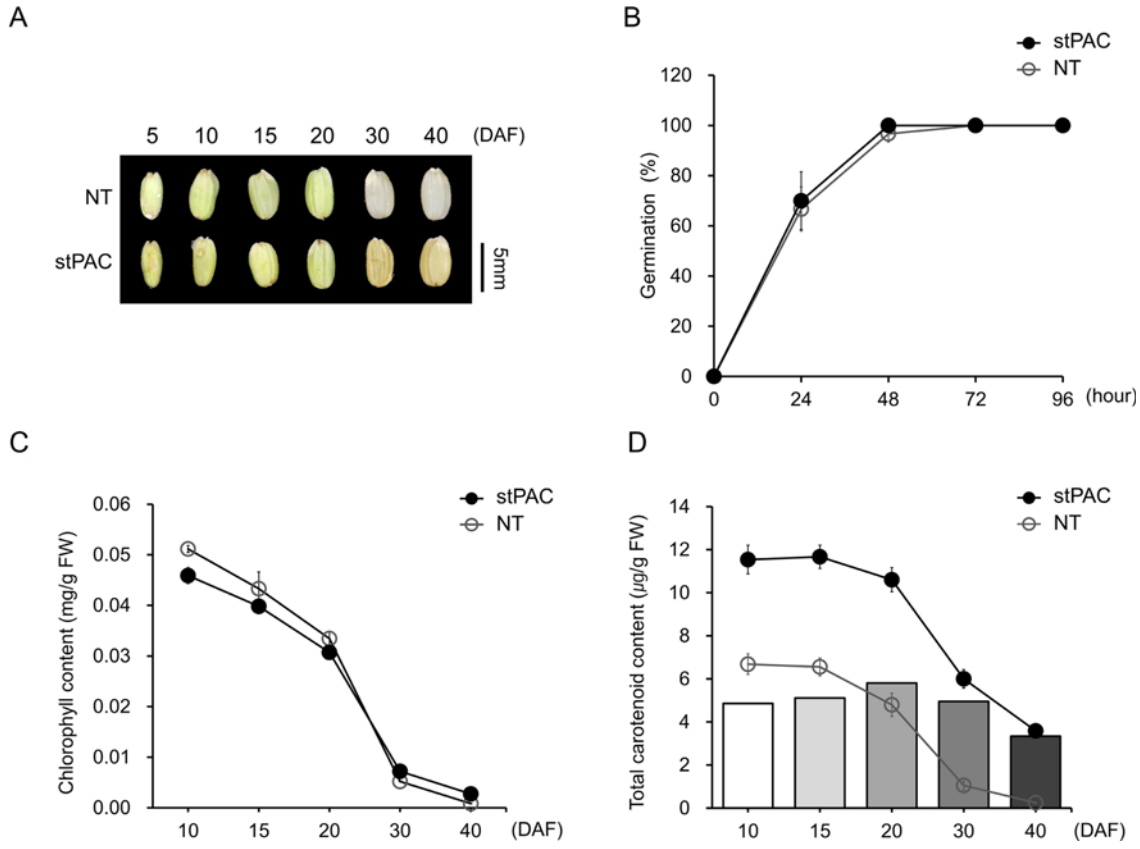

Fig. 2. Phenotype of NT and *stPAC* seeds during development. (A) Photographs showing the color and size phenotypes after dehusking. (B) Germination rate checked in daily intervals (from 24 to 96 hours). Data are mean ± S.D. of three replicates of 10 seeds. (C) Chlorophyll content determined by optical densitometer. (D) Total amounts of carotenoid determined by HPLC. Non-transgenic (NT) and transgenic *stPAC* seeds are represented as open circles and closed circles in B, C and D, respectively. Rectangles indicate the quantitative differences of total carotenoid contents between *stPAC* and NT seeds in D.

both varieties. These carotenoid patterns are similar to those of wheat (Qin et al. 2016) but not sorghum (Kean et al. 2007) and maize (Farr et al. 2013). While carotenoids almost disappeared at 40 DAF in NT grains, substantial amounts of total carotenoids were added by *de novo* production in *stPAC* rice from the beginning stage throughout development as 4.86 μg/g (10 DAF), 5.11 μg/g (15 DAF), 5.81 μg/g (20 DAF), 4.96 μg/g (30 DAF) and 3.34 μg/g (40 DAF), which was 1.7-, 1.8-, 2.2-, 5.7- and 14.4-fold higher relative to NT, respectively (Fig. 2D). The above results indicate that the *stPAC* transgene does not influence grain morphology or metabolisms of GA, ABA and chlorophyll, but only carotenoid metabolism.

Interestingly, the levels of chlorophylls and carotenoids declined the most rapidly between 20 and 30 DAF with the disappearance of green coloration. This could be a transition phase to accelerate and complete the change from chloroplasts into amyloplasts, which are specialized plastids that store starch in rice grains (Howitt and Pogson 2006; Zhai et al. 2016). Due to the lack of specialized lipoprotein-sequestering structures and/or plastoglobuli, amyloplasts might not be considered the proper location for synthesis of or repository for carotenoids (Lopez et al. 2008; Li et al. 2016). Instead, forced carotenogenesis could trigger differentiation of amylo-chromoplast types, which have been discovered in saffron (Grilli Caiola and Canini 2004) and tobacco (Horner et al. 2007) and visualized in rice endosperm (Bai et al. 2016) as similar structures to nest anew-generated plastoglobuli. For deposit of carotenoids in starchy organs, plastoglobuli emerge and then chromoplasts differentiate by carotenoid accumulation above a certain threshold (Howitt and Pogson 2006; Bai et al. 2016).

Individual Carotenoid Profiles During Seed Development

To elucidate how initial carotenoids were altered during the development process, individual carotenoid composition was compared between NT and *stPAC* seeds (Fig. 3; Table S2). Among the eight carotenoids detected, including the acyclic carotenoid lycopene, five β-carotenoids (β-carotene, β-cryptoxanthin, zeaxanthin, antheraxanthin and violaxanthin) and two α-carotenoids (α-carotene and lutein), the main components at 10 DAF were lutein (43.4%) in NT seeds and β-

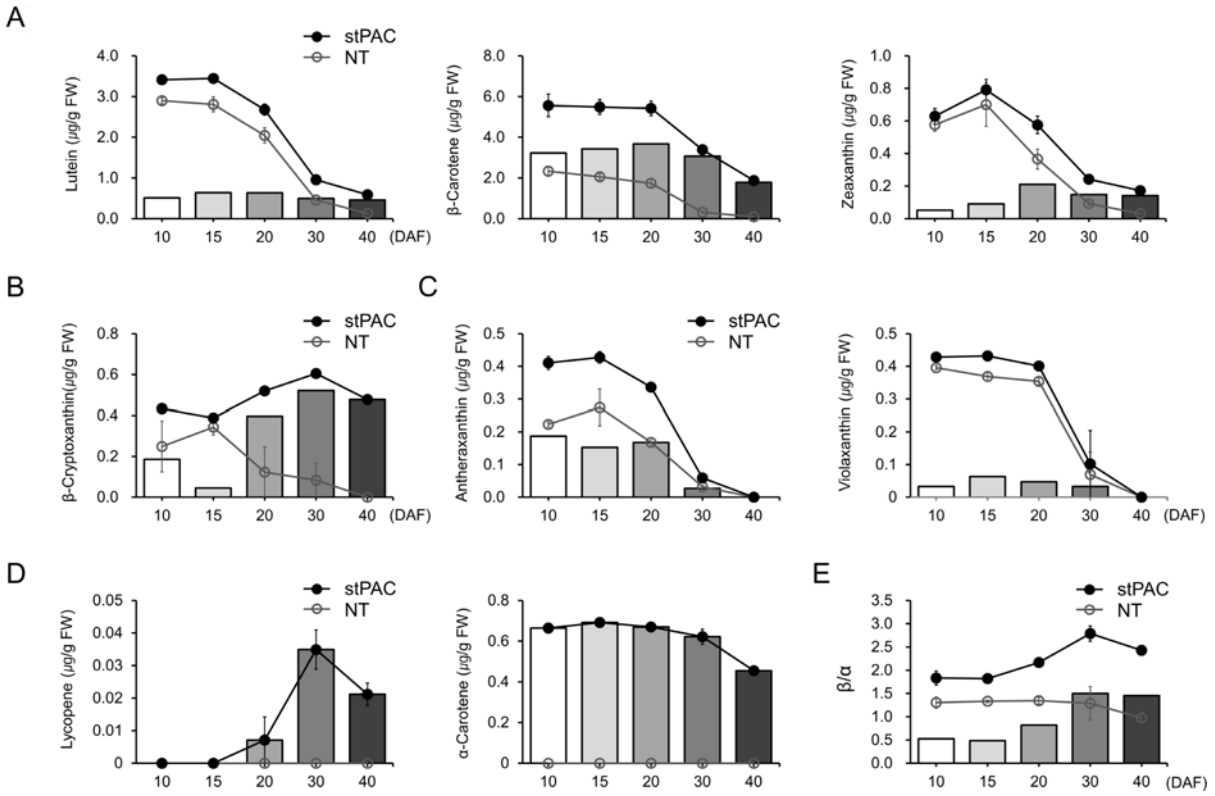

Fig. 3. Comparison of individual carotenoid content between NT and *stPAC* seeds during development. (A) Three major carotenoids, lutein, β-carotene and zeaxanthin, in both rice varieties showing similar patterns to total carotenoids in Fig. 2D. (B) β-cryptoxanthin showing totally differing profiles between NT and *stPAC*. (C) Two carotenoids, antheraxanthin and violaxanthin, vanishing completely at 40 DAF in both rice varieties. (D) Two carotenoids, lycopene and α-carotene, generating and accumulating only in *stPAC*. (E) β/α ratio. The contents of β-carotenoids were expressed as the sum of β-carotene, β-cryptoxanthin, zeaxanthin, antheraxanthin and violaxanthin and α-carotenoids as the sum of α-carotene and lutein. Data are expressed as mean (μg/g fresh weight) ± S.E. from three independent experiments using unpolished seeds. Open and closed circles indicate non-transgenic (NT) and transgenic *stPAC*, respectively, and rectangles indicate the quantitative differences in carotenoid content between *stPAC* and NT seeds.

carotene (48.2%) in *stPAC* seeds (Table S2). In native grain system, the most abundant carotenoid among cereal crops was different during seed development: lutein following by β-carotene as early as stages in wheat (Qin et al. 2016) and zeaxanthin following by lutein in the middle stages of sorghum (Kean et al. 2007) and maize (Farr et al. 2013), implying the distinguished mechanisms of grain carotenogenesis. It suggested that NT rice seeds have the similar carotenoid metabolism to wheat grains but *stPAC* rice seeds have the altered carotenoid metabolism being mainly comprised of β-carotene, lutein and zeaxanthin, which showed the comparable patterns with total carotenoids during seed development (Fig. 3A). β-Cryptoxanthin was decreased and exhausted at 40 DAF in NT but it was increased until 30 DAF and accumulated at 40 DAF in *stPAC* rice (Fig. 3B). Antheraxanthin and violaxanthin were completely depleted at 40 DAF in both varieties, although *stPAC* produced higher levels at early stages of 10 and 20 DAF (Fig. 3C). Lycopene and α-carotene were biosynthesized only in *stPAC* rice with the patterns of a late increase after 20 DAF and consistently high from 10 DAF, respectively (Fig. 3D). These different carotenoid profiles resulted in final compositions in mature seeds at 40 DAF between NT and *stPAC* rice: the 0.25 μg/g of total carotenoids being made up of the three components, lutein (50.7%), β-carotene (37.1%) and zeaxanthin (12.2%), in NT seeds and the 3.59 μg/g of total carotenoids being comprised of the six components, β-carotene (52.3%) as the most significant contributor and followed by lutein (16.3%), β-cryptoxanthin (13.3%), α-carotene (12.7%), zeaxanthin (4.8%) and lycopene (0.6%), in *stPAC* seeds (Fig. 3; Table S2).

Individual composition also largely affected the β/α ratio, which displayed different patterns during seed development between NT and *stPAC* rice (Fig. 3E). In NT rice, the β/α ratio was constant from 10 to 30 DAF and then slightly decreased at 40 DAF, reflecting a larger proportion of lutein at seed maturation. In *stPAC* rice, the β/α ratio was 1.4-fold higher at the beginning stages than in NT rice, increased between 20 and 30 DAF, and then slightly decreased at 40 DAF but was still 2.5-fold higher than in NT rice. This suggested that the b-branch preference of the *stPAC* transgene begins in the early stages and peaks at 30 DAF. Interestingly, the proportion of carotenes to xanthophylls was not remarkably altered from 10 DAF (35:65%) to 40 DAF (36:64%) in NT rice but increased from 10 DAF (54:46%) to 40 DAF (65:35%) in *stPAC* rice. This also indicated that the *stPAC* transgene was more effective in driving the production of carotenes than xanthophylls. It strongly suggested that the host carotenoid metabolism of rice seeds might tightly regulate xanthophyll levels by depleting antheraxanthin and violaxanthin even when their upstream carotenoids are biofortified. Considering that xanthophylls are precursors of ABA, a phytohormone that inhibits cereal seed germination, this was supported by no significant difference in germination rate between NT and *stPAC* seeds as seen in Fig. 2B. Similar results have been reported in carotenoid-biofortified maize studies showing undetectable levels of antheraxanthin at the late stages after a peak in early stages of endosperm development, supporting its status as an ABA precursor (Farr et al. 2013).

Expression Profiles of Transgenes During Seed Development

To elucidate the effect of recombinant *stPAC* gene expression on seed carotenoid metabolism, transcript levels of two bicistronic transgenes, *stPsy* and *stCrtI*, were first defined by qRT-PCR together with rice globulin gene (*OsGlb*), because *stPAC* is expressed under the control of the endosperm-specific *OsGlb* promoter (Qu and Takaiwa 2004) (Fig. 4A). The two transgenes showed similar expression profiles of gradual increase from 10 to 20 DAF and decrease from 20 to 40 DAF, comparable to the *OsGlb* promoter expression. Meanwhile, the *Bar* transgene, an herbicide-tolerant selectable marker under control of a constitutive 35S promoter in an independent cassette, showed higher expression in the earlier stages (Jeong et al. 2017). In addition, protein expression of the *stPAC* transgene was determined by immunoblot using an anti-CRTI antibody (Fig. 4B). It was very low at 10–15 DAF, increased since 20 DAF and more stably accumulated at 40 DAF, suggesting a correlation between transcriptional and translational levels of *stCrtI* since 20 DAF and increased stability of the protein over the mRNA after that.

Taken together, the profiles of carotenoids (Fig. 2D; Fig. 3) and transgene expression (Fig. 4) show that the heterologous biosynthetic pathway in rice seeds fully relies on the seed-specific promoter manner without disturbance by the intrinsic regulation mechanism. This is similar to potato in which carotenoid pathway introduction resulted in a consistent increase in tuber carotenoids associating the transgene expression by tuber-specific *Pat1* promoters, but interfered with leaf carotenogenesis by the constitutive expression under the 35S promoter (Diretto et al. 2007). This suggests that both total and individual carotenoid accumulation are a strictly regulated endogenous mechanism in photosynthetic leaf tissues but not in non-photosynthetic sink tissues like seeds and tubers. In particular, seeds have a strict mechanism to exhaust xanthophylls as substrates for dormancy-related ABA biogenesis at the final stage of maturation (Howitt and Pogson 2006; Farré et al. 2013; Li et al. 2016).

Expression Profiles of Endogenous Carotenoid Metabolic Genes During Seed Development

To unveil the inherent regulatory mechanism of seed carotenoids, transcript levels of 38 endogenous genes involved in

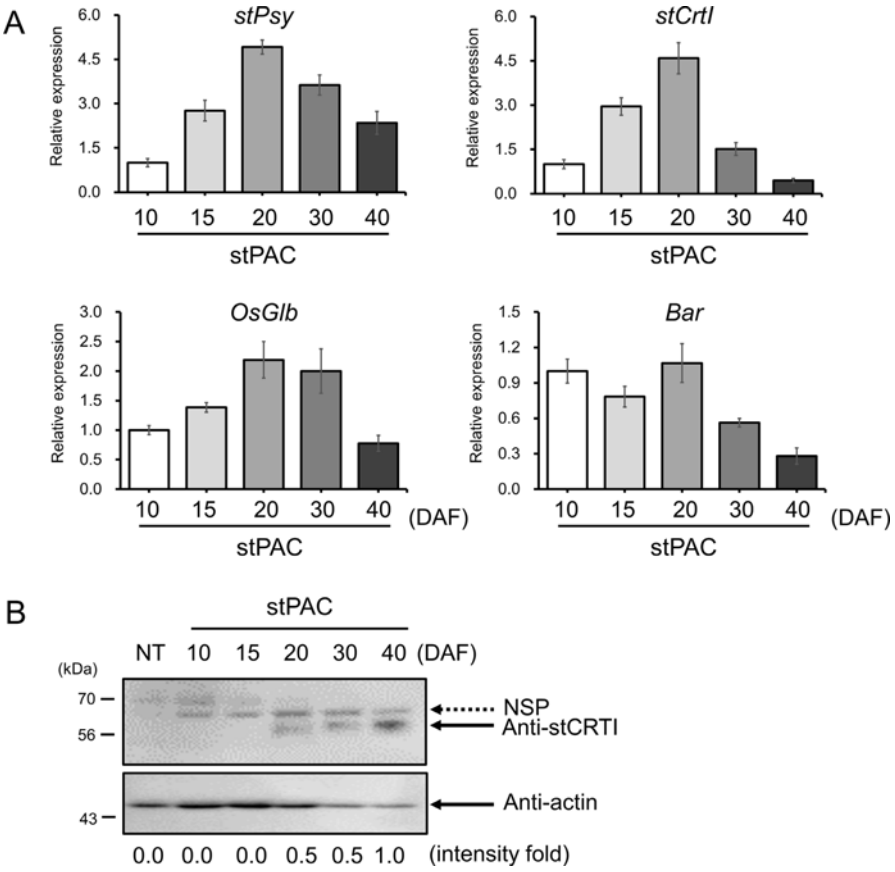

Fig. 4. Expression pattern of the transgenes in *stPAC* seeds during development. (A) Relative expression levels of the transgenes *stPsy*, *stCrtI* and *Bar* and the endogenous *Glb* gene quantified by qRT-PCR. The same amounts of seed RNAs were normalized with the *OsUbi 5* gene. Error bars represent the standard deviations among triplicate experimental reactions. (B) Western blot analysis performed using CRTI antibody in non-transgenic (NT) seeds at 40 DAF and *stPAC* seeds at different developmental stages. The anti-stCRTI and non-specific product (NSP) are indicated by solid and dotted arrows, respectively. Intensity folds of anti-stCRTI were normalized with anti-actin signal and calculated using anti-stCRTI signal at 40 DAF.

carotenoid metabolism including ten for the methylerythritol phosphate (MEP) pathway to supply carotenoid precursor (Fig. 5A), eleven for carotene biosynthesis (Fig. 5B), nine for xanthophyll biosynthesis (Fig. 5C) and eight for carotenoid cleavage dioxygenase (CCD) pathway (Fig. 5D), were compared between NT and *stPAC* seeds according to developmental stages by qRT-PCR. First, in NT seeds, transcripts of six genes, *OsIspG*, *OsGGPS1, OsLCYE, OsBOH1, OsCYP97A* and *OsCYP97C*, showed higher levels at 10−15 DAF and then declined, suggesting they may be involved in the production of chlorophyll-dependent carotenoids at the initial steps of seed development as shown by higher levels of chlorophylls (Fig. 2B). Another 24 genes were gradually up-regulated from low levels at 10 DAF to peak at 30 DAF and then declined at 40 DAF. Eight genes, *OsCYP97B, OsZEP1, OsCCD1, 4b, 8a* and *8b* and *OsNCED1* and *3*, showed the highest expression at 20 DAF. This suggests that carotenoid anabolism is most active at 30 DAF and carotenoid catabolism is active at 20 DAF as well as 30 DAF. Similarly, the decreased transcript levels of 16 carotenoid biosynthetic genes have been reported in mature seeds from the developing seeds of two rice varieties (Chaudhary et al. 2010). Six genes encoding xanthophyll cycle enzymes and CCDs were predominantly and differently expressed in other tissues of either leaf, seedling, root or ovary than embryo and endosperm of seeds, suggesting stringent control of ABA function at the synthetic level in rice seeds (Xue et al. 2012).

On the other hand, *stPAC* seeds showed noticeably different patterns than the NT seeds, which displayed distinct peaks at 30 DAF in most genes (Fig. 5). Although 19 genes showed similarly higher expression at 30 DAF in *stPAC* seeds, they were overall down-regulated as compared with NT seeds, suggesting negative feedback regulation by enhanced carotenoid production. Expression of five genes (*OsDXS3, OsIspD, OsIspG, OsGGPS1* and *OsLYCE*) were delayed and six (*OsDXR, OsIspH1, OsGGPS2, OsZDS, OsLYCB* and *OsCYP97B*) were advanced as compared with the expression timing in NT seeds. Among them, *OsIspG, OsCYP97B* and *OsZEP1* were largely up-regulated with individually altered patterns to be postponed, advanced and

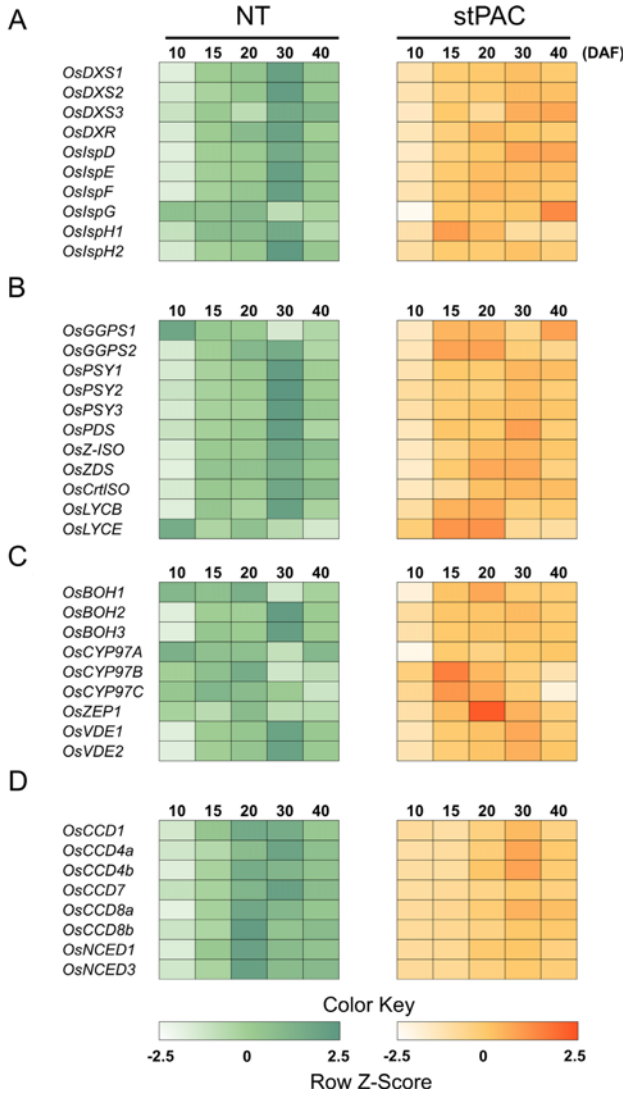

Fig. 5. Quantitative real-time PCR analysis of carotenogenic endogenous genes in NT and *stPAC* seeds during development. (A) Ten methylerythritol phosphate pathway genes for carotenoid precursor supply. (B) Eleven carotene biosynthetic genes. (C) Nine xanthophyll biosynthetic genes. (D) Eight carotenoid cleavage dioxygenase genes. The same amounts of seed RNAs were normalized with the *OsUbi 5* gene. Heatmap shows the *z*-score from differential expression level of genes and relevant down- or up-expression patterns are displayed with different colorimetry as green in NT and orange in *stPAC*, respectively.

maintained, respectively. Two *DXS* genes (*OsDXS1* and *OsDXS2*), three *PSY* genes (*OsPSY1*, *OsPSY2* and *OsPSY3*) and three *BOH* genes (*OsBOH2, OsBOH3* and *OsCYP97A*) were highly suppressed in *stPAC* seeds compared with NT seeds, suggesting that these steps might be important as regulatory points (Fig. 5A-C). *DXS*s and *PSY*s have been known as critical steps in regulation of the capacity for carotenogenesis in several plants including rice (Bai et al. 2016) and the *BCH* gene has also been confirmed as a key player in the petals of *Osmanthus fragrans*, accumulating more β-carotene by low expression of *OfCHYB* in orange-red cultivars and higher proportions of lutein by relatively higher *OfCHYB* expression in yellowish-white cultivars (Wang et al. 2018). The remaining eight *CCD* genes were relatively similarly expressed within 20–30 DAF but entirely delayed to 30 DAF at slightly lower levels in *stPAC* than mainly 20 DAF in NT seeds (Fig. 5D). The *stPAC* transgene altered transcription patterns of endogenous genes relating to substrate supply, biosynthesis and degradation of carotenoids throughout seed development.

Interestingly, the period of high *OsCCDs* expression at 20–30 DAF coincided with a sharp decrease of total and major carotenoids in both NT and *stPAC* (Fig. 2D; Fig. 3A). These associated profiles indicated that this is a turning point at which the balance maintained until 20 DAF between synthesis and degradation of carotenoids by accelerating carotenoid catabolic gene expression after 20 DAF during seed development. The correlation between *CCD* expression level and amounts of carotenoids has been reported in plant seeds (Qin et al. 2016). Hexa- and tetra-ploid wheat grains showed elevated expression of the CCD homologs, *CCD-A4* and *CCD-B4*, in pericarps, while total carotenoids decreased toward the late stages of grain development. Maize *CCD1* was more highly expressed at the beginning of grain development with relatively lower carotenoids in the white variety, suggesting its expression was inversely correlated with accumulation of high contents of carotenoids (Messias et al. 2014). Loss of *AtCCD4* function in Arabidopsis also caused increased accumulation, but not synthesis and deposition, of carotenoids in seeds, suggesting carotenoid catabolism greatly exceeded anabolism during late and desiccation stages of development (Gonzalez-Jorge et al. 2013). This result led to the promising idea to stabilize and increase the level of provitamin A carotenoids by *CCD4* orthologs in seeds of major food crops. This was successfully performed in rice grains to increase carotenoids with a preference toward α-ring or β-ring types by RNAi-mediated suppression of either *OsCCD1* or *OsCCD4a*, proving that *CCD*s act as negative regulators of carotenoid accumulation in crops, too (Ko et al. 2018).

Effect of Prolonged Storage and Pedigree of *stPAC* Seed on Carotenoid Contents

In a previous study, rice bran showed stable levels of carotenoids with lutein as the major component over 10 years of storage at 4°C with the covering hull intact (Belefant-Miller and Grace 2010). Total carotenoid contents in GR grains were not or less reduced in the first two months and then declined 5 to 10% after 5 months of storage at 4°C, with less stability at room temperature (Nghia et al. 2006). Another study showed that β-carotene in GR seeds stored as paddy at ambient temperature during 215 days was degraded with a

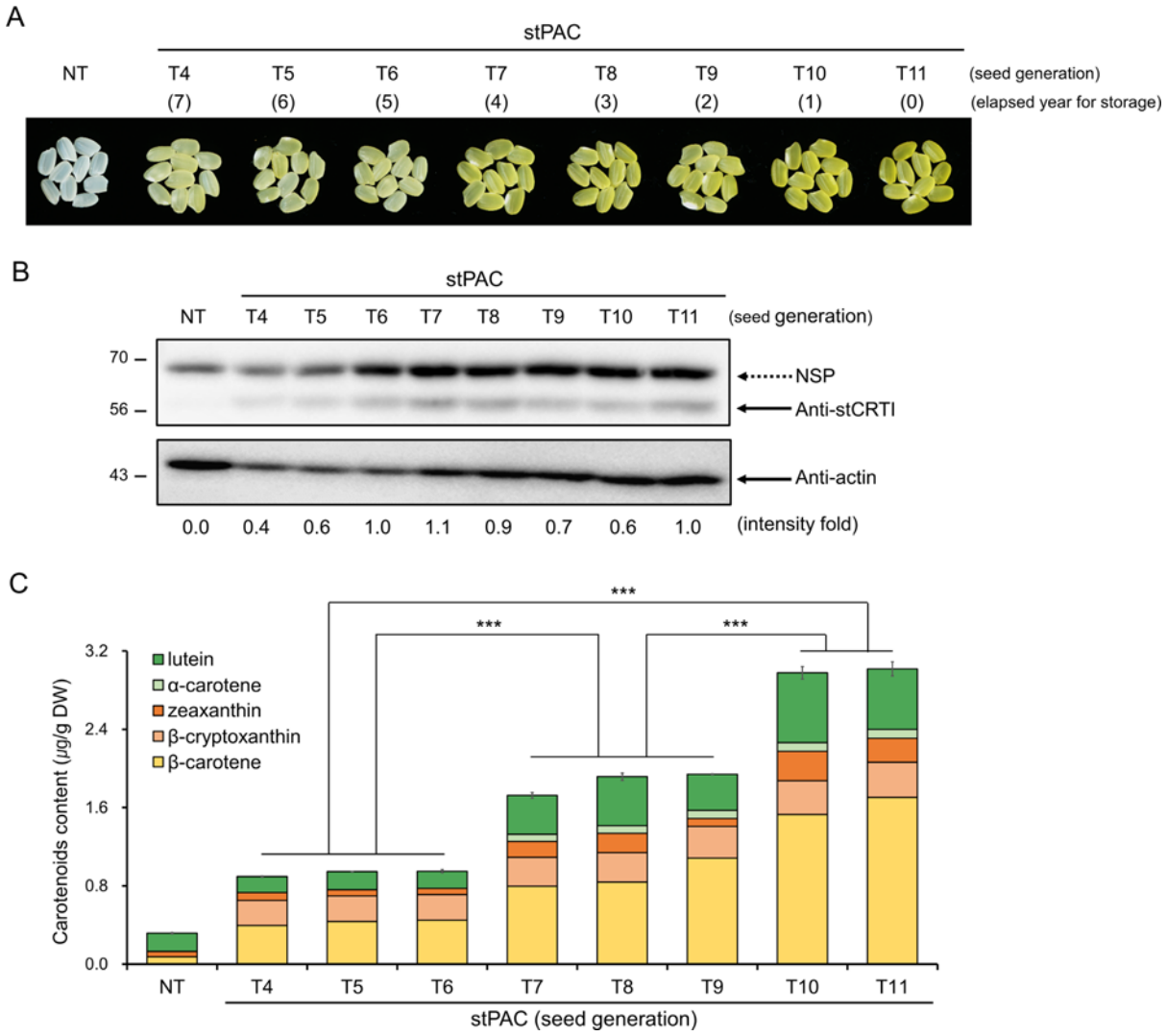

Fig. 6. Stability of biofortified carotenoids in eight consecutive *stPAC* pedigrees during prolonged seed storage. (A) Photographs of eight consecutive generations of polished *stPAC* seeds stored at 18°C for seven years with non-transgenic (NT) seeds. (B) Western blot analysis performed with the same *stPAC* seeds shown in Fig. 6A using CRTI antibody. The anti-stCRTI and non-specific product (NSP) are indicated by solid and dotted arrows, respectively. Intensity folds of anti-stCRTI were normalized with anti-actin signal as loading control and calculated using anti-stCRTI signal at the T11 generation. (C) Total and individual carotenoid contents of the same *stPAC* seeds shown in Fig. 6A are displayed as accumulated bar graph. Statistical significance was calculated via two-tailed Student's *t*-test (*** $p < 0.001$).

half-life of 25 days into β-carotene-derived apocarotenoids, revealing a substantial nonezymatic proportion of β-carotene decay (Schaub et al. 2017).

To evaluate the stability of biofortified carotenoids in rice grains during much longer-term storage, homozygous *stPAC* rice seeds stored at 18°C for seven years were compared in seed color, protein levels and the total contents and composition of carotenoids among eight consecutive pedigrees (Fig. 6). Based on the latest T11 generation of *stPAC* seeds grown in the paddy field in 2018, yellow coloration faded in three steps: T11 to T10, T9 to T7 and T6 to T4, indicating a stepwise loss of colorful carotenoids during prolonged storage (Fig. 6A). Meanwhile, CRTI protein, the transgene product, was similarly accumulated more between T11 and T6 than T5 and T4, suggesting stability within 5-year storage (Fig. 6B). Interestingly, in a pattern consistent with seed color, total carotenoid contents remained unchanged for one year of T11 to T10, significantly decreased from 64 to 57% between 2–4 years of T9 to T7 and then largely decreased from 32 to 30% between 5–7 years of T6 to T4 during prolonged seed storage (Fig. 6C). As the *stPAC* seeds were stored longer, contents of β-carotene, zeaxanthin and lutein at T11 were decreased by 23%, 33% and 26%, respectively, at T4 with a similar pattern to total carotenoids. α-Carotene was eventually disappeared after five years of seed storage and β-cryptoxanthin remained by 72% with relatively less

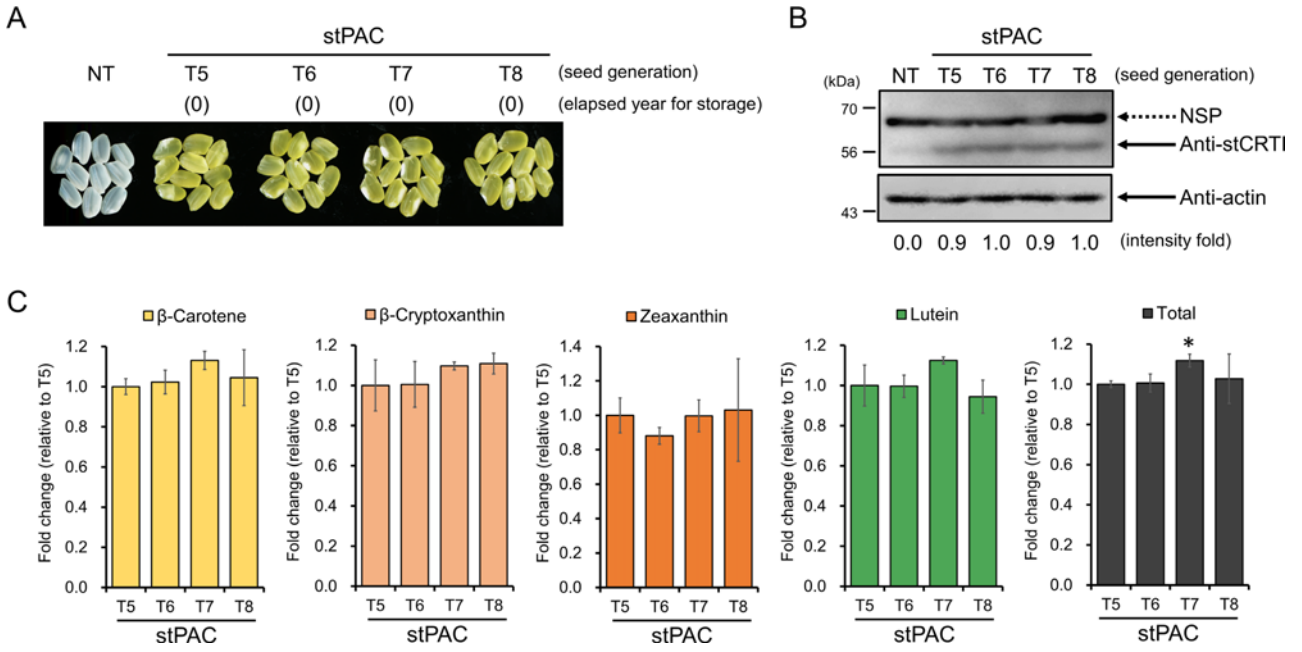

Fig. 7. Stability of biofortified carotenoids in four simultaneously re-grown *stPAC* pedigrees. (A) Photographs of four consecutive generation of polished seeds of *stPAC* progenies re-grown in the same field conditions with non-transgenic (NT) seeds. (B) Western blot analysis performed with the same *stPAC* seeds shown in Fig. 7A using CRTI antibody. The anti-stCRTI and non-specific product (NSP) are indicated by solid and dotted arrows, respectively. Intensity folds of anti-stCRTI were normalized with anti-actin signal as loading control and calculated using anti-stCRTI signal at the T8 generation as a reference 1. (C) Each and total carotenoid levels at different generations are expressed as the fold changes relative to those at the T8 generation. Statistical significance was calculated via two-tailed Student's *t*-test (*$p < 0.05$).

decomposition until the T4 generation, indicating its higher stability than other components during seed storage.

To examine the cause of the decrease in carotenoid contents under long-term seed storage, four *stPAC* seeds at T4, T5, T6 and T7 were simultaneously re-grown in the same field to minimize environmental effects. Progeny seeds at T5, T6, T7 and T8 showed similar yellow coloration, CRTI protein accumulation and total and individual carotenoid contents, with T7 seeds being slightly higher (Fig. 7A-C). This complete restoration to the same levels corroborated that the carotenoid loss during seed storage might be caused by not damage in production ability but chemical and physical degradation. Our results show that the *stPAC* gene was inheritably transmitted, stably expressed and consistently enriched β-carotene as a main component up to T11, suggesting the reliability of a genetically introduced carotenoid pathway under long-term storage of rice grains.

Materials and Methods

Rice Grain Materials

Seeds of transgenic *stPAC* (*stPsy-2A-stCrtI*) rice with the golden-colored trait (Jeong et al. 2017) and its background non-transgenic (NT) rice (*Oryza sativa* L. cv. Hwayoung) were sprouted for 1 week on Murashige–Skoog (MS) agar medium in a growth chamber after sterilization with 70% ethanol and 2% sodium hypochlorite. These plantlets were transferred into soil in the greenhouse at 28°C for 4 weeks and then transplanted into the field and grown during the summer season until maturity. Rice seeds were harvested at six developmental stages of 5, 10, 15, 20, 30 and 40 days after flowering (DAF) and their coloration was visually inspected after carefully removing the husks with forceps. The fresh seeds were immediately frozen in liquid nitrogen and stored at -80°C for extraction of metabolites, RNAs and proteins. Some were oven-dried at 65°C for 48 h to compare weight and moisture content using an electronic balance. The germination rate of dried seeds was examined for four days in a growth chamber under continuous dark at 28°C. The homozygous *stPAC* seeds with continuous lineages were harvested yearly and kept in long-term storage at 18ºC and below 40% relative humidity without light. The *stPAC* plants in four consecutive generations of T4, T5, T6, and T7 were simultaneously grown with T10 plants to harvest their seed progenies under the same field conditions.

Analysis of Chlorophylls and Carotenoids

Chlorophylls were extracted from rice grain powder by gently mixing at 500 rpm in 100% methanol at 70ºC for 30 min with a Thermomixer (Eppendorf AG, Hamburg, Germany) followed by centrifugation at 800 × g and 4ºC for 10 min. The quantification was performed after absorbance measurement at 660 and 653 nm with an Optizen POP spectrophotometer (Mecasys Co., Daejeon, Republic of Korea) and calculated as previously described (Song et al. 2016). Total contents were expressed as the sum of chlorophyll *a* and *b*.

Carotenoids were also extracted from rice grain powder and prepared for high-performance liquid chromatography (HPLC) analysis as described previously (Jeong et al. 2017; Ha et al. 2019).

Carotenoids were then separated on a C30 YMC column (3 μm, 4.6 × 250 mm, YMC Co., Kyoto, Japan) using an Agilent 1100 series HPLC system (Agilent, Massy, France) under the gradient elution conditions described previously (Ha et al. 2019). For quantification, the peak areas of HPLC chromatograms generated at 450 nm were determined relative to those of the calibration curves, which were drawn by plotting the peak area ratios with the *β*-apo-8'-carotenal (Sigma-Aldrich Chemical Com. St. Louis, MO, USA). Individual carotenoid component was identified by their distinctive retention time and their contents were calculated using ten respective standards: lycopene (*ψ,ψ*-carotene), *α*-carotene (*β,ε*-carotene), 13*Z*-*β*-carotene, (all-*E*)-*β*-carotene, 9*Z*-*β*-carotene, lutein (*β,ε*-carotene-diol), β-cryptoxanthin [(3R)-*β,β*-carotene-diol], zeaxanthin (*β,β*-carotene-diol), antheraxanthin [(3S,5R,6S,3'R)-5,6-epoxy-5,6-dihydro-*β,β*-carotene-3,3'-diol] and violaxanthin [(3S,5R,6S,3'S,5'R,6'S)-5,6:5',6'-diepoxy-5,6,5',6'-tetrahydro-*β,β*-carotene-3,3'-diol] (all from CaroteNature, Lupsingen, Switzerland). Amount of β-carotene was calculated as the sum of 13*Z*-*β*-carotene, (all-*E*)-*β*-carotene and 9*Z*-*β*-carotene and that of total carotenoids as the sum of each carotenoid content. Data from three independent biological replicates were analyzed and differences between groups were determined using the unpaired student's *t*-test. A p value less than 0.05 was judged statistically significant.

RNA Analysis

Total RNAs were extracted from the rice grains with the PureLink® Plant RNA Reagent (Invitrogen, Waltham, MA, USA) according to the manufacturer's instructions. The remaining genomic DNAs were removed by treatment with RNase-free DNase I (Qiagen, Hilden, Germany) and RNA quality was checked at 260/280 nm by a NanoDrop Spectrophotometer ND-2000 (NanoDrop Technologies, Wilmington, DE, USA). cDNAs were simultaneously synthesized and amplified from 1 μg of total RNAs using AccuPower® RT Premix according to the manufacturer's instructions (Bioneer, Daejeon, Republic of Korea). Quantitative real-time PCR (qRT-PCR) analyses were performed with CFX Connect™ Real-Time PCR Detection System (Bio-Rad, Richmond, CA, USA). Each reaction contained 20 ng of template cDNA, 0.3 μM of each gene-specific primer pair and 10 μl SYBR Green Real-Time PCR Master Mix (Bio-Rad) in a total volume of 20 μl. PCR conditions were an initial incubation at 95°C for 3 min followed by 40 cycles of 95°C for 15 s and 60°C for 30 s. Melting curve analysis was performed at the end to confirm proper amplification of target transcripts. Baseline and threshold cycles (Ct value) were automatically calculated using default parameters. The rice *Ubiquitin5* gene (Os01g22490) was used as a reference to normalize and minimize variation in cDNA template levels. Quantification of transcripts was determined with three independent biological replicates using the standard curve method. Primer sequences in their respective genes used for qRT-PCR are listed in Table S1.

Protein Analysis

Proteins were extracted from the rice grains using buffer containing 0.025M Tris-HCl (pH 6.8), 4% SDS, 4M Urea and 5% 2-mercaptoethanol for 30 min and centrifuged at 12,000g for 45 min at 4ºC. Protein concentration was determined using Quant-iT™ Protein Assay Kit (Invitrogen). A total of 40 μg of proteins were electrophoresed on an 8% SDS/polyacrylamide gel and transferred onto a PVDF membrane (Whatman, Kent, UK) using a Trans-Blot SD Semi-Dry electrophoretic transfer cell (Bio-Rad). Immuno-blotting was performed using primary anti-CRTI antibody (kindly provided by Dr. Peter Beyer group at University of Freiburg in Germany) raised against *Pantoea* CRTI protein. Plant-actin antibody (Cusabio Technology LLC, Houston, TX, USA) was used as loading control. Antibody-bound signals were developed using anti-rabbit IgG (Fc) alkaline phosphatase-conjugated secondary antibody (Promega, Madison, WI, USA), imaged using the LAS 4000 software (Fujifilm, Kanagawa, Japan) and quantified with ImageJ software (National Institute of Health, http://rsb.info.nih.gov/ij/).

Acknowledgements

This work was supported by grants from the Next-Generation BioGreen 21 Program (PJ01368801 and PJ01334601 to S.-H. Ha) funded by the Rural Development Administration.

Author's Contributions

JKK and S-HH designed the experiments; YSJ, YJJ, MKY, TJK, S-HL and JKK performed the experiments; H-KK, YSJ, and S-HH analyzed the data; H-KK and S-HH wrote the paper. All authors reviewed and approved the final manuscript.

Supporting Information

Fig. S1. Physiological characterization of NT and *stPAC* seeds.
Table S1. Primers used in this study.
Table S2. The content and composition of chlorophyll and carotenoid during rice seed development.
Table S3. Expression levels of endogenous carotenoid metabolic genes during rice see development.

References

Badejo AA (2018) Elevated carotenoids in staple crops: The biosynthesis, challenges and measures for target delivery. J Genet Eng Biotechnol 16:553–562

Bai C, Capell T, Berman J, Medina V, Sandmann G, Christou P, Zhu C (2016) Bottlenecks in carotenoid biosynthesis and accumulation in rice endosperm are influenced by the precursor-product balance. Plant Biotechnol J 14:195–205

Belefant-Miller H, Grace SC (2010) Variations in bran carotenoid levels within and between rice subgroups. Plant Food Hum Nutr 65:358–363

Cao S, Liang M, Shi L, Shao J, Song C, Bian K, Chen W, Yang Z (2017) Accumulation of carotenoids and expression of carotenogenic genes in peach fruit. Food Chem 214:137-146

Chaudhary N, Nijhawan A, Khurana JP, Khurana P (2010) Carotenoid biosynthesis genes in rice: structural analysis, genome-wide expression profiling and phylogenetic analysis. Mol Genet Genomics 283:13–33

Diretto G, Al-Babili S, Tavazza R, Papacchioli V, Beyer P, Giuliano G (2007) Metabolic engineering of potato carotenoid content through tuber-specific overexpression of a bacterial mini-pathway. PLoS One 2:e350

Eggersdorfer M, Wyss A (2018) Carotenoids in human nutrition and health. Arch Biochem Biophys 652:18–26

Emiliani J, D'Andrea L, Lorena Falcone Ferreyra M, Maulión E, Rodriguez E, Rodriguez-Concepción M, Casati P (2018) A role for β,β-xanthophylls in Arabidopsis UV-B photoprotection. J Exp Bot 69:4921–4933

Farré G, Maiam Rivera S, Alves R, Vilaprinyo E, Sorribas A, Canela R, Naqvi S, Sandmann G, Capell T, Zhu C, Christou P (2013)

Targeted transcriptomic and metabolic profiling reveals temporal bottlenecks in the maize carotenoid pathway that may be addressed by multigene engineering. Plant J 75:441–455
Fiedor J, Burda K (2014) Potential role of carotenoids as antioxidants in human health and disease. Nutrients 6:466–488
Fitzpatrick TB, Basset GJ, Borel P, Carrari F, DellaPenna D, Fraser PD, Hellmann H, Osorio S, Rothan C, Valpuesta V, Caris-Veyrat C, Fernie AR (2012) Vitamin deficiencies in humans: can plant science help? Plant Cell 24:395–414
Fraser PD, Truesdale MR, Bird CR, Schuch W, Bramley PM (1994) Carotenoid biosynthesis during tomato fruit development (evidence for tissue-specific gene expression). Plant Physiol 105:405–413
Gayen D, Ghosh S, Paul S, Sarkar SN, Datta SK, Datta K (2016) Metabolic regulation of carotenoid-enriched Golden Rice line. Front Plant Sci 7:1622
Gonzalez-Jorge S, Ha S-H, Magallanes-Lundback M, Gilliland LU, Zhou A, Lipka AE, Nguyen Y, Angelovici R, Lin H, Cepela J, Little H, Buell CR, Gore MA, DellaPenna D (2013) Carotenoid cleavage dioxygenase4 Is a negative regulator of beta-carotene content in Arabidopsis seeds. Plant Cell 25:4812–4826
Grilli Caiola M, Canini A (2004) Ultrastructure of chromoplasts and other plastids in *Crocus sativus* L. (Iridaceae). Plant Biosyst 138:43–52
Ha S-H, Kim JK, Jeong YS, You MK, Lim SH, Kim J-K (2019) Stepwise pathway engineering to the biosynthesis of zeaxanthin, astaxanthin and capsanthin in rice endosperm. Metab Eng 52:178–189
Ha S-H, Liang YS, Jung H, Ahn M-J, Suh S-C, Kweon S-J, Kim D-H, Kim Y-M, Kim J-K (2010) Application of two bicistronic systems involving 2A and IRES sequences to the biosynthesis of carotenoids in rice endosperm. Plant Biotechnol J 8:928–938
Hadjipieri M, Georgiadou EC, Marin A, Diaz-Mula HM, Goulas V, Fotopoulos V, Tomas-Barberan FA, Manganaris GA (2017) Metabolic and transcriptional elucidation of the carotenoid biosynthesis pathway in peel and flesh tissue of loquat fruit during on-tree development. BMC Plant Biol 17:102
Hashimoto H, Uragami C, Cogdell RJ (2016) Carotenoids and photosynthesis. Subcell Biochem 79:111–139
Horner HT, Healy RA, Ren G, Fritz D, Klyne A, Seames C, Thornburg RW (2007) Amyloplast to chromoplast conversion in developing ornamental tobacco floral nectaries provides sugar for nectar and antioxidants for protection. Am J Bot 94:12–24
Hou X, Rivers J, Leon P, McQuinn RP, Pogson BJ (2016) Synthesis and function of apocarotenoid signals in plants. Trends Plant Sci 21:792–803
Howitt CA, Pogson BJ (2006) Carotenoid accumulation and function in seeds and non-green tissues. Plant Cell Environ 29:435–445
Jeong YS, Ku H-K, Kim JK, You MK, Lim SH, Kim J-K, Ha S-H (2017) Effect of codon optimization on the enhancement of the β-carotene contents in rice endosperm. Plant Biotechnol Rep 11:171–179
Karppinen K, Zoratti L, Sarala M, Carvalho E, Hirsimaki J, Mentula H, Martens S, Haggman H, Jaakola L (2016) Carotenoid metabolism during bilberry (*Vaccinium myrtillus* L.) fruit development under different light conditions is regulated by biosynthesis and degradation. BMC Plant Biol 16:95
Kean EG, Ejeta G, Hamaker BR, Ferruzzi MG (2007) Characterization of carotenoid pigments in mature and developing kernels of selected yellow-endosperm sorghum varieties. J Agric Food Chem 55:2619–2626
Ko MR, Song MH, Kim JK, Baek SA, You MK, Lim SH, Ha S-H (2018) RNAi-mediated suppression of three carotenoid-cleavage dioxygenase genes, OsCCD1, 4a, and 4b, increases carotenoid content in rice. J Exp Bot 69:5105–5116
Li L, Yuan H, Zeng Y, Xu Q (2016) Plastids and carotenoid accumulation. Subcell Biochem 79:273–293
Lopez AB, Yang Y, Thannhauser TW, Li L (2008) Phytoene desaturase is present in a large protein complex in the plastid membrane. Physiol Plant 133:190–198
Lv P, Li N, Liu H, Gu H, Zhao W (2015) Changes in carotenoid profiles and in the expression pattern of the genes in carotenoid metabolisms during fruit development and ripening in four watermelon cultivars. Food Chem 174:52–59
Messias RdS, Galli V, dos Anjos e Silva, Sergio Delmar, Rombaldi CV (2014) Carotenoid biosynthetic and catabolic pathways: gene expression and carotenoid content in grains of maize landraces. Nutrients 6:546–563
Nghia PT, Liem DT, Hai TV, Hoa TTC (2006) Effect of storage conditions on total carotenoid content in golden rice grains. Omonrice 14:18–27
Paine JA, Shipton CA, Chaggar S, Howells RM, Kennedy MJ, Vernon G, Wright SY, Hinchliffe E, Adams JL, Silverstone AL, Drake R (2005) Improving the nutritional value of Golden Rice through increased pro-vitamin A content. Nat Biotechnol 23:482–487
Qin X, Fischer K, Yu S, Dubcovsky J, Tian L (2016) Distinct expression and function of carotenoid metabolic genes and homoeologs in developing wheat grains. BMC Plant Biol 16:155
Qu LQ, Takaiwa F (2004) Evaluation of tissue specificity and expression strength of rice seed component gene promoters in transgenic rice. Plant Biotechnol J 2:113–125
Rodriguez-Concepcion M, Avalos J, Bonet ML, Boronat A, Gomez-Gomez L, Hornero-Mendez D, Limon MC, Meléndez-Martínez AJ, Olmedilla-Alonso B, Palou A, Ribot J, Rodrigo MJ, Zacarias L, Zhu C (2018) A global perspective on carotenoids: Metabolism, biotechnology, and benefits for nutrition and health. Prog Lipid Res 70:62–93
Sayre R, Beeching JR, Cahoon EB, Egesi C, Fauquet C, Fellman J, Fregene M, Gruissem W, Mallowa S, Manary M, Maziya-Dixon B, Mbanaso A, Schachtman DP, Siritunga D, Taylor N, Vanderschuren H, Zhang P (2011) The BioCassava plus program: biofortification of cassava for sub-Saharan Africa. Annu Rev Plant Bio 62:251–272
Schaub P, Al-Babili S, Drake R, Beyer P (2005) Why is golden rice golden (yellow) instead of red? Plant Physiol 138:441–450
Schaub P, Wust F, Koschmieder J, Yu Q, Virk P, Tohme J, Beyer P (2017) Nonenzymatic beta-carotene degradation in provitamin A-biofortified crop plants. J Agric Food Chem 65:6588–6598
Song MH, Lim SH, Kim JK, Jung ES, John KM, You MK, Ahn SN, Lee CH, Ha S-H (2016) In planta cleavage of carotenoids by Arabidopsis carotenoid cleavage dioxygenase 4 in transgenic rice plants. Plant Biotechnol Rep 10:291–300
Wang Y, Zhang C, Dong B, Fu J, Hu S, Zhao H (2018) Carotenoid accumulation and its contribution to flower coloration of *Osmanthus fragrans*. Front Plant Sci 9:1499
Xue L, Zhang J, Xue H (2012) Genome-wide analysis of the complex transcriptional networks of rice developing seeds. PLoS One 7:e31081
Ye X, Al-Babili S, Kloti A, Zhang J, Lucca P, Beyer P, Potrykus I (2000) Engineering the provitamin A (beta-carotene) biosynthetic pathway into (carotenoid-free) rice endosperm. Science 287:303–305
Zeng J, Wang X, Miao Y, Wang C, Zang M, Chen X, Li M, Li X, Wang Q, Li K, Chang J, Wang Y, Yang G, He G (2015) Metabolic engineering of wheat provitamin A by simultaneously overexpressing CrtB and silencing carotenoid hydroxylase (TaHYD). J Agric Food Chem 63:9083–9092
Zhai S, Xia X, He Z (2016) Carotenoids in staple cereals: metabolism, regulation, and genetic manipulation. Front Plant Sci 7:1197
Zhu C, Naqvi S, Breitenbach J, Sandmann G, Christou P, Capell T (2008) Combinatorial genetic transformation generates a library of metabolic phenotypes for the carotenoid pathway in maize. Proc Natl Acad Sci USA 105:18232–18237